Numerical integration of the equations of motion of structural systems undergoing large 3D rotations: dynamics of corotational slender beam elements

Francesco Foti · Luca Martinelli · Federico Perotti

Received: 15 February 2014 / Accepted: 27 June 2014 / Published online: 22 July 2014

1 Introduction

This paper deals with the numerical simulation of the dynamic response of frame structures undergoing large three-dimensional (3D) rotations and displacements, but small strains. This is a largely studied topic in the fields of flexible multibody and structural mechanics (e.g. [31]).

Amongst the results in the literature, geometrically non-linear beam finite elements (FE) have been based on the geometrically exact (GE) approach and the corotational (CR) one. GE elements have the advantage of an exact description of the beam kinematics. Most implementations are based on the hypothesis of the material being hyperelastic, e.g. [4, 8, 27, 28], while only few deal with nonlinear material behavior, e.g. [21, 22]. This is, in fact, not a trivial problem to solve, requiring the development of ad hoc non-linear constitutive laws in terms of finite strain measures. CR elements are based on the decomposition [14] of the total motion in a rigid part and in an approximately pure deformational one by introducing an element-attached local, or "corotated", reference system. The element response is first evaluated in the corotated system and subsequently transformed into the global system. The decomposition is defined, in "element independent" CR formulations ([14, 26]) only on the basis of the element "topology".

Compared to the GE approach, the main advantage of the CR formulation is the ability to adopt stress and strain measures that otherwise would result in non-objective formulations when large displacements and rotations occur. This is particularly useful in view of the introduction of non-linear and, more generally, inelastic constitutive laws (one of the forecasted

F. Foti (✉) · L. Martinelli · F. Perotti
Dipartimento di Ingegneria Civile e Ambientale, Politecnico di Milano, Piazza L. da Vinci 32, 20132 Milano, Italy
e-mail: francesco.foti@polimi.it

developments of this research). In addition, the CR approach has the practical advantage of allowing for "reusing" at the local level proved existing libraries of small displacement-small strains FEs.

CR beam formulations have been largely adopted to study instability problems [2, 25]; only few works focused on the dynamic response (e.g. [7, 17, 18]). In fact, the total motion decomposition of CR elements leads to cumbersome expressions of the inertia forces, with coupling terms between the local deformational kinematic variables and the global variables representing the rigid body motion of the corotated reference system (e.g. [17]). This aspect was addressed by Crisfield and coworkers in [7] where a classic CR formulation was adopted to evaluate the internal (restoring) forces, while inertia forces were defined starting from a an exact description of the cross section kinematics. However, differently from GE formulations, translation variables were defined, and interpolated, in the global (inertial) reference system of the problem while angular velocity and acceleration of the cross section were first transformed into the corotated reference system and then interpolated. As a result, some kinematic nodal variables were defined in the global reference system, and some others in the corotated one, implying an ad hoc time stepping algorithm.

Taking this approach a step further, in this work a formulation is proposed based on the hypothesis of arbitrarily large nodal displacements and 3D rotations, while strains are assumed small in a local (corotated) reference system. At the local level, a classic Euler–Bernoulli beam formulation is adopted for the restoring forces. On the other hand, a different model is adopted for inertia forces. These are evaluated starting from an expression of the kinetic energy which employs only nodal variables defined in the global reference system, thus avoiding the complications stemming from the decomposition of the total motion at the element level. To preserve the element-independent character of the approach, special care is devoted to ensure that all procedures depending on a particular choice of rotation parameters are performed outside the element. In fact, a crucial issue in the modelling flexible structures undergoing large displacements is the representation of 3D rotations, due to their non commutative character. Rotations do not belong to a linear space and cannot be composed as vectors; to account for these aspects, modified versions of the Newmark time stepping scheme have been proposed (e.g. [4, 19, 29]). In this work a parametrization of the rotation group is adopted based on the exponential map and the rotation vector. The proposed procedure allows for an additive update of the rotation parameters with practical advantages on the reuse of standard Newmark time stepping schemes.

2 Kinematics of large rotations: a summary

From a strictly mathematical point of view, a rotation can be regarded as a linear transformation of the oriented 3D Euclidean vector space E^3 onto itself, which doesn't affect the metric and the orientation of the space. As it is well known, the only mappings satisfying these requirements are the proper (or *special*) orthogonal tensors: $\boldsymbol{\Lambda}$: $E^3 \rightarrow E^3$. They can be collected into a set and equipped with the usual definition of tensor product to obtain the non-commutative group of rotations, usually denoted as $SO(3)$.

Denoting as $\boldsymbol{I}$ the identity tensor, the following statement can be introduced:

$$SO(3) = \left\{ \boldsymbol{\Lambda} : E^3 \rightarrow E^3, linear | \boldsymbol{\Lambda}\boldsymbol{\Lambda}^T = \boldsymbol{I}, \det(\boldsymbol{\Lambda}) = 1 \right\} \tag{1}$$

The rotation group is also a non linear differential manifold with dimension three, e.g. [5, 20]. Hence, a local description of $SO(3)$ can be obtained by introducing a three-parameter chart. Several mapping strategies have been adopted in literature, a comprehensive review of which can be found in [15]. Here the focus is on a parametrization based on the rotation vector $\boldsymbol{\phi} = \{\phi_1, \phi_2, \phi_3\}^T$ and the exponential map:

$$\boldsymbol{\Lambda} = \exp(\boldsymbol{S}(\boldsymbol{\phi})) = \sum_{k=0}^{\infty} \frac{1}{k!} \boldsymbol{S}^k(\boldsymbol{\phi}) \tag{2}$$

where $\boldsymbol{S}(\boldsymbol{\phi})$ is a skew-symmetric tensor whose components are related to those of the rotation vector as follows:

$$\boldsymbol{S}(\boldsymbol{\phi}) = \begin{pmatrix} 0 & -\phi_3 & \phi_2 \\ \phi_3 & 0 & -\phi_1 \\ -\phi_2 & \phi_1 & 0 \end{pmatrix} \tag{3}$$

As it can be shown by means of simple geometrical arguments (e.g. [1]), denoting as $\| \cdot \|$ the Euclidean norm of a vector, the following closed form expression holds:

$$\boldsymbol{\Lambda}(\boldsymbol{\phi}) = \boldsymbol{I} + \frac{\sin\|\boldsymbol{\phi}\|}{\|\boldsymbol{\phi}\|}\boldsymbol{S}(\boldsymbol{\phi}) + \frac{(1-\cos\|\boldsymbol{\phi}\|)}{\|\boldsymbol{\phi}\|^2}\boldsymbol{S}^2(\boldsymbol{\phi}) \tag{4}$$

Approximate expressions can also be obtained by truncated series expansions, e.g. [1, 6]. The following first and second order approximations are here considered for sake of comparison:

$$\boldsymbol{\Lambda}(\boldsymbol{\phi}) = \boldsymbol{I} + \boldsymbol{S}(\boldsymbol{\phi}) \tag{5}$$

$$\boldsymbol{\Lambda}(\boldsymbol{\phi}) = \boldsymbol{I} + \left[\boldsymbol{S}(\boldsymbol{\phi}) + \frac{1}{2}\boldsymbol{S}^2(\boldsymbol{\phi})\right] \Big/ \left(1 + \frac{1}{4}\boldsymbol{\phi}^T\boldsymbol{\phi}\right) \tag{6}$$

By definition, the result of a group operation is still an element of the group. So, given a generic pair of elements: $\boldsymbol{\Lambda}_1, \boldsymbol{\Lambda}_2 \in SO(3)$, it's always possible to define a third element, in the following denoted as incremental rotation tensor, $\boldsymbol{\Lambda}_{inc}$, which allows to transform $\boldsymbol{\Lambda}_1$ into $\boldsymbol{\Lambda}_2$ as a result of the group operation. Due to the non-commutative character of the group operation this tensor, however, is not unique. In fact, we can distinguish between a *left-* and a *right-*application of the incremental rotation tensor. The corresponding tensors will be respectively characterized by the superscript *'L'* or *'R'*. Then, the following holds:

$$\boldsymbol{\Lambda}_2 = \boldsymbol{\Lambda}^L_{inc}\boldsymbol{\Lambda}_1 = \boldsymbol{\Lambda}_1\boldsymbol{\Lambda}^R_{inc} \tag{7}$$

The above expression provides a means to evaluate compound rotations. Indeed, the application of the left- (right-) incremental rotation tensor can be regarded as the mathematical description of a superimposed rotation about fixed (follower) axes in space, so allowing for a spatial (material) description of a rotational motion.

In the following we will only focus on a spatial description of the rotational motion. Within this context, denoting as $so(3)$ the set of skew-symmetric tensors defined by Eq. (3), the tangent space at a generic point $\boldsymbol{\Lambda}$ (base point) of $SO(3)$ can be introduced as follows (see e.g. [20] for a more detailed discussion on this topic):

$$T_{\Lambda}SO(3) = \{\boldsymbol{S}\boldsymbol{\Lambda} | \boldsymbol{\Lambda} \in SO(3), \quad \boldsymbol{S} \in so(3)\} \tag{8}$$

With a slight abuse of terminology, we will refer to the incremental rotation vectors, i.e. rotation vectors related through (2) to an incremental rotation tensor, as elements of $T_{\Lambda}SO(3)$. This choice is motivated because the linear composition of incremental rotations referred to the same base point gives results in $T_{\Lambda}SO(3)$. In fact, denoting with $\boldsymbol{\theta}_1$ and $\boldsymbol{\theta}_2$ two incremental rotation vectors from $\boldsymbol{\Lambda}$, the following holds:

$$\boldsymbol{S}(\alpha\boldsymbol{\theta}_1)\boldsymbol{\Lambda} + \boldsymbol{S}(\beta\boldsymbol{\theta}_2)\boldsymbol{\Lambda} = \boldsymbol{S}(\alpha\boldsymbol{\theta}_1 + \beta\boldsymbol{\theta}_2)\boldsymbol{\Lambda}, \forall\alpha, \beta \in \mathbb{R} \tag{9}$$

Similarly, it's possible to show that the rotation vector $\boldsymbol{\phi}$ belongs to the tangent space with base point at the identity tensor $\boldsymbol{I}$, here denoted as: $T_ISO(3)$. Hence, vectors $\boldsymbol{\theta}$ and $\boldsymbol{\phi}$ belong to different tangent spaces. As a consequence, they cannot be linearly composed, even in the limit case of small incremental rotations (i.e. $\boldsymbol{\theta} \to \boldsymbol{0}$). However, a non-linear relationship between variations can be expressed by introducing the tangential transformation tensor, $\boldsymbol{H}(\boldsymbol{\phi})$ (whose expression can be found e.g. in [20]), as follows:

$$\delta\boldsymbol{\theta} = \boldsymbol{H}(\boldsymbol{\phi})\delta\boldsymbol{\phi} \tag{10}$$

Considering a rigid body, and denoting as $\{\boldsymbol{a}_i\}$, $(i = 1, 2, 3)$, the set of unit vectors of a body-attached right handed Cartesian frame, the orientation of the body during its motion with respect to a fixed reference system can be described through a rotation tensor $\boldsymbol{\Lambda}$, which is a function of a time variable t. Denoting as $\{\boldsymbol{E}_i\}$, $(i = 1, 2, 3)$, the set of unit vectors of a right handed Cartesian frame associated to the global reference system, the following holds:

$$\boldsymbol{a}_i(t) = \boldsymbol{\Lambda}(t)\boldsymbol{E}_i, \; i = 1, 2, 3 \tag{11}$$

The spatial representation of the angular velocity, $\boldsymbol{\omega}$, and of the angular acceleration, $\boldsymbol{\alpha}$, of the body, then, satisfies the following relationships, where the dot denotes derivation with respect to time:

$$\boldsymbol{S}(\boldsymbol{\omega}) = \dot{\boldsymbol{\Lambda}}\boldsymbol{\Lambda}^T \tag{12}$$

$$\boldsymbol{S}(\boldsymbol{\alpha}) = \dot{\boldsymbol{\Lambda}}\dot{\boldsymbol{\Lambda}}^T + \ddot{\boldsymbol{\Lambda}}\boldsymbol{\Lambda}^T \tag{13}$$

It can be shown [20] that the angular velocity and acceleration vectors belong to the tangent space $T_{\Lambda}SO(3)$. However, they can be evaluated as a function of the time derivatives of the rotation vector, which belong to $T_ISO(3)$. To this aim, the following non-linear relationships are here introduced:

$$\boldsymbol{\omega} = \boldsymbol{H}(\boldsymbol{\phi})\dot{\boldsymbol{\phi}} \tag{14}$$

$$\boldsymbol{\alpha} = \boldsymbol{H}(\boldsymbol{\phi})\ddot{\boldsymbol{\phi}} + \dot{\boldsymbol{H}}(\boldsymbol{\phi}, \dot{\boldsymbol{\phi}})\dot{\boldsymbol{\phi}} \tag{15}$$

where $\dot{\boldsymbol{H}}(\boldsymbol{\phi}, \dot{\boldsymbol{\phi}})$ denotes the time-derivative tensor of $\boldsymbol{H}(\boldsymbol{\phi})$ (whose expression can be found e.g. in [20]).

3 The corotational beam element: statics

The basic idea of the corotational approach is to decompose the total motion of a finite element into a rigid body motion and an approximately pure deformational contribution. This is obtained by introducing a local, or corotated, reference frame (CRF) which continuously translates and rotates, following the motion of the element. Consistently, in the implementation here proposed, internal forces are evaluated first in the local frame, where the additional hypothesis of small strains is adopted, and then transformed into the global reference system.

The local response of the element is described according to the classic Euler–Bernoulli beam theory, so neglecting shear and warping effects. For simplicity, we consider here elements with constant cross sections and an initially straight centerline. The kinematic variables at the local level are measured with respect to the axes: x_1, x_2, x_3, defined in the local reference configuration of the mechanical problem such that: x_1 is the chord axis of the element, x_2 and x_3 are the principal axes of the cross sections. Accordingly, we define the local deformational generalized displacements (shown in Fig. 1 together to the associated generalized forces) as the flexural end rotations $\theta_i^{(j)}$, with $i = 1, 2$, and $j = 2, 3$ (the subscript refers to the node, the superscript to the axis of rotation—x_2 or x_3—in the CRF), the total twist (relative rotation of member ends), θ_t; and the relative axial displacement, e. Local displacements are collected into the column matrix:

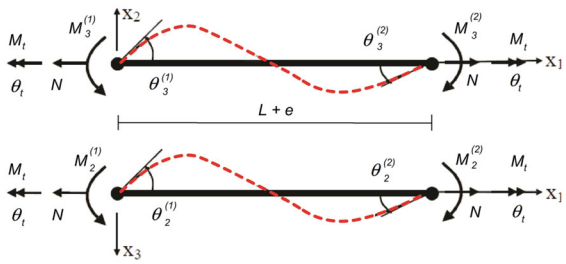

Fig. 1 Member displacements and forces in the corotated reference frame

$$\boldsymbol{p} = \left(e, \theta_t, \theta_2^{(1)}, \theta_3^{(1)}, \theta_2^{(2)}, \theta_3^{(2)}\right)^T \tag{16}$$

Cubic shape functions are adopted for lateral displacements, while a linear interpolation is assumed for twist and axial displacement. The axial strain at each section is defined taking into account the low order non linearity due to the effect of bending (bowing effect). The element forces, which are collected into the column matrix:

$$\boldsymbol{P} = \left(N, M_t, M_2^{(1)}, M_3^{(1)}, M_2^{(2)}, M_3^{(2)}\right)^T \tag{17}$$

and the tangent stiffness matrix, $\boldsymbol{K}_{loc} = \frac{\partial \boldsymbol{P}}{\partial \boldsymbol{p}}$, at the local level can be easily derived in closed form in the hypothesis of linearly-elastic material, or by means of numerical integration. In this second, more general, case, attention should be paid to avoid membrane locking due to the linear interpolation of the relative axial elongation (see e.g. [6]).

3.1 Update of nodes configuration

With reference to the two node beam element, schematically represented in Fig. 2, the configuration of its nodes is fully defined by their position and orientation with respect to a reference system, here the global one whose axes are directed as the unit vectors of the basis $\{\boldsymbol{E}_i\}$, $(i = 1, 2, 3)$. For node $j = 1, 2$, the configuration is given by the position vectors $\boldsymbol{X}^{(j)}$, $(i = 1, 2, 3)$, and a node-attached right handed Cartesian system, defined by the set of unit vectors: $\left\{\boldsymbol{a}_i^{(j)}\right\}$ $(i = 1, 2, 3,$ and $j = 1, 2)$. According to Eq. (11), the latter are completely defined in the current configuration by the nodal rotation tensors $\boldsymbol{\Lambda}^{(j)}$. Within the context of an incremental analysis, the kinematic of nodes is described by adopting an updated Lagrangian approach. Denoting with the subscript '*old*' the variables referred to the last converged step of the analysis, and defining $\Delta\boldsymbol{d}^{(j)}$ the incremental translation vector of the j-th node, position vectors are updated as follows:

$$\boldsymbol{X}^{(j)} = \boldsymbol{X}_{old}^{(j)} + \Delta\boldsymbol{d}^{(j)}, j = 1, 2 \tag{18}$$

The orientation of the nodes is similarly updated by exploiting the spatial description of compound rotations [Eq. (7)]. Denoting as $\boldsymbol{\Lambda}_{inc}^{(j)}$ the incremental

rotation tensor of the j-th node, the following updating expression can be used:

$$\boldsymbol{\Lambda}^{(j)} = \boldsymbol{\Lambda}_{inc}^{(j)} \boldsymbol{\Lambda}_{old}^{(j)}, j = 1, 2 \tag{19}$$

It's worth noting that the procedure here adopted for the update of the nodal configuration is formally independent from both the local element formulation and the particular parametrization of nodal rotations. In this work, however, a parametrization based on the rotation vector has been adopted. Then, the generalized displacements of the element in the global reference frame are the nodal translation vectors $\boldsymbol{d}^{(j)}$ and the rotation vectors $\boldsymbol{\phi}^{(j)}$, related to the j-th nodal rotation tensor through the exponential map of $SO(3)$. They can be conveniently collected into the column matrix:

$$\boldsymbol{q} = \left(\boldsymbol{q}_d^T, \boldsymbol{q}_r^T\right)^T = \left(\boldsymbol{d}_1^T, \boldsymbol{d}_2^T, \boldsymbol{\varphi}_1^T, \boldsymbol{\varphi}_2^T\right)^T \tag{20}$$

For comparative purposes, three different strategies have been considered for the evaluation of the incremental rotation tensor which appear in Eq. (7), starting from the knowledge of the nodal incremental rotation. They are based on the complete trigonometric expression (4) and the approximations introduced in (5) and (6).We refer to these procedures respectively as: *closed form updated Lagrangian* (CFUL), *first-order updated Lagrangian* (FOUL) and *second-order updated Lagrangian* (SOUL). The validity of FOUL is limited to small (i.e. infinitesimal) rotations increments. This hypothesis is relaxed in the SOUL procedure and totally removed in the CFUL approach, based on the complete (trigonometric) expression of the rotation tensor.

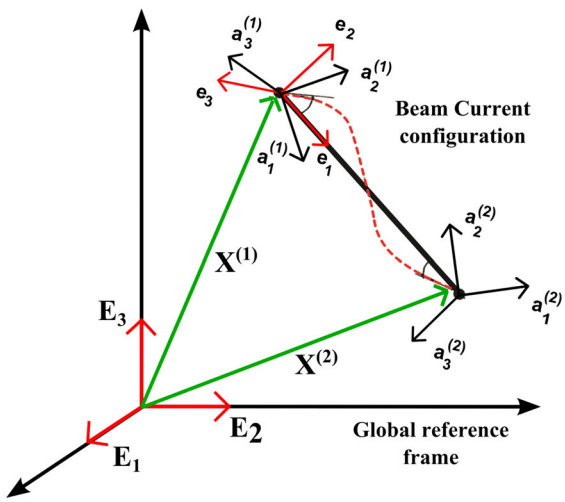

Fig. 2 3D corotational beam element. Current configuration

3.2 Local reference frame orientation

Once the current nodes configuration is known, the local corotated reference frame of the element can be defined. To this end, several formulations are currently available in literature, as shown in [14] and references therein. Here we assume as starting point the approach presented first by Oran in [24] and later adopted by Meek and Tan in [23], which has been furhter developed by the authors research group to study the mechanical response of cable stuctures (e.g.: [9–11, 13]).

This work, however, departs substantially from the aforementioned formulation. In fact this can take into account large nodal displacements and rotations, but its validity is restricted to the small increments hypothesis for the nodal rotations. The assumed smallness of nodal rotation increments was recognized as a consequence of:

- the update strategy of the joint orientation matrices, which is based on a first order approximate expression of the nodal incremental rotation matrices;
- the update strategy of the node orientation matrices, which is based on a first order approximate expression of the nodal incremental rotation matrices;
- the procedure for the evaluation of the generalized nodal forces, which is not fully consistent to the virtual work principle.

On the contrary, our approach relies on a general (and element-independent) description of large nodal rotations, able to recover the small increments hypothesis as a special case (i.e. FOUL rotation update procedure). Moreover the global generalized forces are defined by exploiting the principle of virtual works, so circumventing also the second drawback of the original formulation. At the very end, we retain from the original formulation only the kinematic relations adopted to define the CRF, which are also rewritten in a slightly different form, more suitable for our further developments.

Making reference to Fig. 2, the local corotated reference frame is attached to the first node of the

element and characterized by the unit vectors $\{\boldsymbol{e}_i\}$, $i = 1, 2, 3$. The first unit vector is directed as the chord of the element:

$$\boldsymbol{e}_1 = \frac{\boldsymbol{X}^{(2)} - \boldsymbol{X}^{(1)}}{\left\|\boldsymbol{X}^{(2)} - \boldsymbol{X}^{(1)}\right\|} \tag{21}$$

The remaining unit vectors $\boldsymbol{e}_2$ and $\boldsymbol{e}_3$ are assumed parallel to the directions of the average principal axes of the cross-sections of the beam. Their directions are thus evaluated, in the reference configuration, by simply processing the input data regarding the geometry of the structural elements. So we can easily calculate and store in memory the initial rotation matrix: $\boldsymbol{\Lambda}_{e0}$, also referred as reference element orientation matrix.

In order to conventionally define the average principal axes of the cross-sections of the beam at a generic current configuration two auxiliary Cartesian frames, attached to the centroids of the end section of the element are then introduced. Their Cartesian bases, here denoted as $\left\{\boldsymbol{b}_i^{(j)}\right\}$, ($i = 1, 2, 3$, and $j = 1, 2$), are evaluated by rotating the reference element orientation matrix by the same angles as the ones defining the nodal rotation matrices.

Finally, $\boldsymbol{e}_2$ and $\boldsymbol{e}_3$ are defined as:

$$2\boldsymbol{e}_2 = \boldsymbol{b}_2^{(1)} + \boldsymbol{b}_2^{(2)} - \left(\boldsymbol{b}_2^{(1)T}\boldsymbol{e}_1\right)\boldsymbol{b}_1^{(1)} - \left(\boldsymbol{b}_2^{(2)T}\boldsymbol{e}_1\right)\boldsymbol{b}_1^{(2)} \tag{22}$$

$$2\boldsymbol{e}_3 = \boldsymbol{b}_3^{(1)} + \boldsymbol{b}_3^{(2)} - \left(\boldsymbol{b}_3^{(1)T}\boldsymbol{e}_1\right)\boldsymbol{b}_1^{(1)} - \left(\boldsymbol{b}_3^{(2)T}\boldsymbol{e}_1\right)\boldsymbol{b}_1^{(2)} \tag{23}$$

It's easy to observe that the physical motivation behind the expressions above is simply the averaging of the directions of the principal inertia axes of the end cross sections. In fact the terms inside the parentheses in (22) and (23) are nothing but the angles defined by the principal axes of the end cross-sections with respect to the chord of the element.

Once the corotated reference frame is defined it's possible to express the local generalized displacements, according to the formulation adopted to describe the mechanical response of the element. The axial relative displacement is obtained as the difference between the current and the reference length of the chord, while the torsional and the flexural rotations are defined as follows:

$$\theta_t = \boldsymbol{b}_3^{(1)T}\boldsymbol{b}_2^{(2)} = \boldsymbol{b}_2^{(1)T}\boldsymbol{b}_3^{(2)} \tag{24}$$

$$\theta_i^{(j)} = k\,\boldsymbol{b}_{i+k}^{(j)T}\boldsymbol{e}_1, j = 1, 2,\ i = 2, 3,\ k = (-1)^i \tag{25}$$

The virtual variation of the local displacements, $\delta\boldsymbol{p}$, is obtained starting from the above expressions and considering a virtual variation of the configuration of the nodes. To this end, we introduce the column matrix:

$$\delta\boldsymbol{q} = \left(\delta\boldsymbol{d}_1{}^T,\ \delta\boldsymbol{d}_2{}^T,\ \delta\boldsymbol{\phi}_1{}^T,\ \delta\boldsymbol{\phi}_2{}^T\right)^T \tag{26}$$

where: $\delta\boldsymbol{d}_1$ and $\delta\boldsymbol{d}_2$ are the variations of the nodal translation vectors, while $\delta\boldsymbol{\phi}_1$ and $\delta\boldsymbol{\phi}_2$ are the variations of the nodal rotation vectors related to the nodal orientation tensors through the exponential map of $SO(3)$. The relationship between $\delta\boldsymbol{p}$ and $\delta\boldsymbol{q}$ can be expressed in matrix form as:

$$\delta\boldsymbol{p} = \boldsymbol{T}\delta\boldsymbol{q} \tag{27}$$

The expression of the corotational transformation matrix, $\boldsymbol{T}$, first derived in closed form by one of the authors in [13] , is given in Appendix.

3.3 Internal forces and tangent stiffness matrix

The internal forces and the tangent stiffness matrix are evaluated by following the consistent approach proposed by Crisfield in [6]. By comparing the expressions of the virtual work in the CRF and in the global reference systems, the nodal generalized internal forces, here collected into the column matrix $\boldsymbol{Q}$, are defined as:

$$\boldsymbol{Q} = \boldsymbol{T}^T\boldsymbol{P} \tag{28}$$

From the previous expression, the tangent stiffness matrix of the element is then derived as:

$$\boldsymbol{K} = \frac{\partial\boldsymbol{Q}}{\partial\boldsymbol{q}} = \boldsymbol{T}^T\boldsymbol{K}_{loc}\boldsymbol{T} + \frac{\partial\boldsymbol{T}^T}{\partial\boldsymbol{q}}\boldsymbol{P} \tag{29}$$

The above matrix is, in general, not symmetric. A symmetric approximation of (29) has been derived in a previous work by one of the authors in [13], under the further hypothesis of symmetry of the local tangent stiffness matrix of the element. The symmetric approximation delivered, within the procedure shown in [13], the same response as the original non symmetric matrix. Nevertheless the latter has been retained in the present work.

4 The corotational beam element: dynamics

The generalized inertia forces acting on a discrete structural system can be defined through a standard application of the Hamilton's principle, starting from an expression of its kinetic energy as a function of its generalized displacements and their time derivatives. Obviously, this also applies for a generic stand-alone beam finite element, whose kinetic energy can be formally expressed as: $T = T(\boldsymbol{q}, \dot{\boldsymbol{q}})$, where $\boldsymbol{q}$ is the generalized displacement vector and $\dot{\boldsymbol{q}}$ is its derivative with respect to the time variable t.

In fact, classic corotational formulations, e.g. [17], employ displacement and velocity fields defined first in the corotated (local) reference system of the element and then transformed back to the inertial (global) one. According to the decomposition of motion into a rigid and an approximately deformational contribution, local displacements and velocities are, in general, non-linear functions of $\boldsymbol{q}$ and $\dot{\boldsymbol{q}}$. This finally leads to very cumbersome calculations in order to evaluate the element inertia forces, especially when rotation parameters appear within $\boldsymbol{q}$, such as for 3D beam elements. Moreover this approach is intimately related to the particular procedure adopted to define the corotated frame and to describe finite rotations.

Departing from these formulations, here inertia forces are evaluated from an expression of the kinetic energy which employs directly nodal variables defined in the inertial reference system, thus avoiding the complications deriving from the decomposition of the total motion at the element level. For structural theories adopting only displacements as kinematic variables this is, of course, a trivial task. On the contrary, when also rotations are involved in the generalized displacement fields, special care should be devoted to ensure that all procedures depending on a particular choice of rotation parameters are performed outside the element formulation. In fact, this is a basic requirement to formally ensure the independence of the approach from the formulation of the local element, the definition of the corotated frame and the parametrization of rotations.

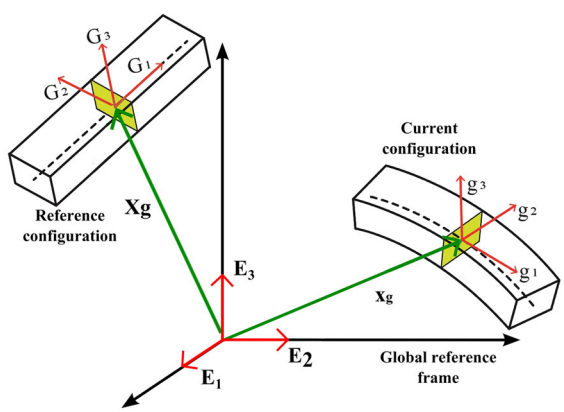

Fig. 3 Beam element in the inertial reference system

Under the plane section assumption, the motion of a generic cross section can be described within the global inertial reference system by introducing a local right handed Cartesian frame rigidly attached to its centroid. Reserving capital letters to identify quantities in the reference configuration of the beam, we denote as $\boldsymbol{x}_g(S,t)$ and $\{\boldsymbol{g}_i(S,t)\}$ respectively the centroid position vector and the local frame unit vectors of a section identified by the arc length coordinate $S \in [0, L]$, where L is the undeformed length of the element. As depicted in Fig. 3, the vector $\boldsymbol{g}_1$ is normal to the plane of the section while $\boldsymbol{g}_2$ and $\boldsymbol{g}_3$ are assumed as parallel to the principal axes. The orientation of the local frame with respect to the inertial one is described by introducing the rotation tensor: $\boldsymbol{\Lambda}(S,t) \in SO(3)$.

The inertial properties of the cross-section are defined through the mass per unit length $m(S)$ of the centerline and the mass moment of inertia tensor $\boldsymbol{J}(S)$. The latter is characterized as the diagonal matrix of components in the sectional attached reference frame: $diag(J_2 + J_3, J_2, J_3)$, where J_2 and J_3 are the principal moment of inertia of the section.

Denoting as $\boldsymbol{\omega}(S,t)$ the angular velocity and as $\boldsymbol{d}(S,t) = \boldsymbol{x}_g(S,t) - \boldsymbol{X}_g(S,t)$ the translation vector of a cross section of the beam, the kinetic energy per unit of length of the beam can be expressed, by summing the contributions of the translation and rotation of a cross section, as it follows:

$$T = T_{tra} + T_{rot} = \frac{1}{2} m(S) \dot{\boldsymbol{d}}(S,t)^T \dot{\boldsymbol{d}}(S,t) + \frac{1}{2} \boldsymbol{\omega}(S,t)^T \boldsymbol{\Lambda}(S,t) \boldsymbol{J}(S) \boldsymbol{\Lambda}(S,t)^T \boldsymbol{\omega}(S,t) \tag{30}$$

The generalized nodal inertia forces, here referred as $\boldsymbol{Q_I}$, can be defined by exploiting the Hamilton's principle as:

$$\delta \boldsymbol{q}^T \boldsymbol{Q}_I = \int_0^L \delta \boldsymbol{q}^T \left(-\frac{d}{dt}\left[\frac{\partial T}{\partial \dot{\boldsymbol{q}}}\right] + \frac{\partial T}{\partial \boldsymbol{q}} \right) dS \tag{31}$$

From the above expression, we get:

$$\delta \boldsymbol{q}^T \boldsymbol{Q}_I = \int_0^L m \delta \boldsymbol{d}^T \ddot{\boldsymbol{d}} dS + \int_0^L \delta \boldsymbol{\theta}^T \left(\boldsymbol{\omega} \times \boldsymbol{\Lambda} \boldsymbol{J} \boldsymbol{\Lambda}^T \boldsymbol{\omega} + \boldsymbol{\Lambda} \boldsymbol{J} \boldsymbol{\Lambda}^T \boldsymbol{\alpha} \right) dS \tag{32}$$

The above equation is adopted to define the inertia forces $\boldsymbol{Q_I}$. To this end, we first evaluate the nodal incremental rotations, $\delta \boldsymbol{\theta}_j$, the nodal incremental angular velocities, $\boldsymbol{\omega}_j$, and the nodal incremental angular accelerations $\boldsymbol{\alpha}_j$, as functions of the nodal rotation pseudo-vectors and of its time derivatives. Recalling Eqs. (10), (14) and (15), we get:

$$\delta \boldsymbol{\theta}_j = \boldsymbol{H}(\boldsymbol{\phi}_j) \delta \boldsymbol{\phi}_j \tag{33}$$

$$\boldsymbol{\omega}_j = \boldsymbol{H}(\boldsymbol{\phi}_j) \dot{\boldsymbol{\phi}}_j \tag{34}$$

$$\boldsymbol{\alpha}_j = \boldsymbol{H}(\boldsymbol{\phi}_j) \ddot{\boldsymbol{\phi}}_j + \dot{\boldsymbol{H}}(\boldsymbol{\phi}_j, \dot{\boldsymbol{\phi}}_j) \dot{\boldsymbol{\phi}}_j \tag{35}$$

where the matrix $\boldsymbol{H}$ and its time derivative have been introduced in Sect. 2.

Note that the above calculations are performed outside the element formulation; thus they are independent of the particular formulation adopted to describe the kinematics of the element itself.

Now, we can interpolate the virtual displacement fields which appear in (32) and the sectional angular velocities and accelerations (33–35) with the following linear functions:

$$\tilde{\psi}_1(S) = \frac{S}{L}, \; \tilde{\psi}_2(S) = 1 - \frac{S}{L}, \text{with} S \in [0, L] \tag{36}$$

In order to evaluate (32), we need the expression of the rotation matrix $\boldsymbol{\Lambda}(S,t)$ at a generic abscissa S. We observe, in this respect, that the spatial interpolation of finite rotations is not a trivial issue, due to the non-linear character of $SO(3)$ e.g. [20]. Moreover, we are here interested in a formulation which is not dependent from the particular choice of the element and rotation parameters employed to describe large nodal rotations.

To this end, let us now assume as known the rotation matrices of nodes, $\boldsymbol{\Lambda}^{(j)}$, and the rotation matrix $\boldsymbol{\Lambda}_e$ which gives the orientation of the corotated reference system with respect to the inertial one. The relative rotation between the j-th node and the corotated frame can be described through an incremental rotation tensor, $\boldsymbol{U}^{(j)}$, according to the spatial description of compound rotations provided in Sect. 2. Within this context, Eq. (7), is rewritten as follows:

$$\boldsymbol{\Lambda}^{(j)}(t) = \boldsymbol{U}^{(j)}(t) \boldsymbol{\Lambda}_e(t), \text{with} \quad j = 1, 2 \tag{37}$$

Then, recalling the orthonormality of the rotation tensors:

$$\boldsymbol{U}^{(j)}(t) = \boldsymbol{\Lambda}^{(j)}(t) \boldsymbol{\Lambda}_e(t)^T, \text{with} \quad j = 1, 2 \tag{38}$$

It's worth noting that through (38) we physically decompose the total rotation of nodes into the contribution of the CRF, which in principle is arbitrarily large, and a relative rotation with respect to the CRF which, in the spirit of the corotational approach, should be small.

Once (38) has been evaluated at each node of the element, the rotation pseudo-vectors can be extracted from the nodal matrices $\boldsymbol{U}^{(j)}$ by adopting, for example, the well known Spurrier's algorithm [30]. Given the previous remark, these pseudo-vectors represent small nodal rotations with respect to the CRF. Formally it is possible to write:

$$\boldsymbol{U}^{(j)}(t) \rightarrow \boldsymbol{\varphi}_{uj}(t) \tag{39}$$

The rotation vectors obtained by (39) can now be easily interpolated:

$$\boldsymbol{\phi}_u(S,t) = \sum_{j=1}^{2} \tilde{\psi}_j(S) \boldsymbol{\phi}_{uj}(t) \tag{40}$$

and at a generic point of the element the rotation matrix, associated to the pseudo vectors (38), it can be calculated by means of the exponential map (2). Formally we can write:

$$\boldsymbol{\phi}_u(S,t) \rightarrow \boldsymbol{U}(S,t) \tag{41}$$

From the map (41) the approximate rotation matrix at a generic point of the element can be evaluated as:

$$\boldsymbol{\Lambda}(S,t) = \boldsymbol{U}(S,t) \boldsymbol{\Lambda}_e(t) \tag{42}$$

It's worth noting that the procedure defined from (37) to (42) behaves as a black-box, once we provide in input the nodal rotation matrices and the CRF orientation matrix. Thus it applies, in principle, for any choice of nodal rotation parameters and for any

corotational finite element.

Finally, according to the partition of the generalized displacement vector of the element introduced in Eq. (20), we can express the element non-linear nodal inertia forces as:

$$\boldsymbol{Q}_I = -\begin{pmatrix} \int_0^L \tilde{\boldsymbol{\Psi}}^T \tilde{\boldsymbol{\Psi}} m(s) dS\, \ddot{\boldsymbol{q}}_d \\ \tilde{\boldsymbol{H}}_R{}^T \int_0^L \tilde{\boldsymbol{\Psi}}^T \left(\boldsymbol{\omega} \times \boldsymbol{\Lambda} \boldsymbol{J} \boldsymbol{\Lambda}^T \boldsymbol{\omega} + \boldsymbol{J} \boldsymbol{\alpha}\right) dS \end{pmatrix} \tag{43}$$

where the following definition has been introduced:

$$\tilde{\boldsymbol{\Psi}}(S) = \begin{pmatrix} \tilde{\psi}_1(S) & 0 \\ 0 & \tilde{\psi}_2(S) \end{pmatrix} \tag{44}$$

and the nodal matrices $\boldsymbol{H}(\phi_j)$ have been collected into the (6×6) block-diagonal matrix $\boldsymbol{H}_R$:

$$\tilde{\boldsymbol{H}}_R = \begin{pmatrix} \boldsymbol{H}(\boldsymbol{\phi}_1) & \boldsymbol{0} \\ \boldsymbol{0} & \boldsymbol{H}(\boldsymbol{\phi}_2) \end{pmatrix} \tag{45}$$

The rotational part in (43) is evaluated in practice by means of a Gauss-Lobatto numerical integration scheme.

Consistent tangent operators can be obtained by linearizing the expression of the inertia force of the element, so obtaining the mass, gyroscopic and centrifugal stiffness matrices [13]. However, as a reasonable simplification we can neglect the gyroscopic and centrifugal stiffness contribution in the evaluation of the tangent operator of an implicit algorithm for the numerical integration of the equations of motions.

As a final remark we observe that the equations of motion of the structural system obtained from the finite element discretization define a set of ordinary differential equation on a non-linear differentiable manifold. Several authors have addressed this interesting problem, both in the applied mathematics field, as in the mechanical one. Modified versions of the Newmark time stepping scheme were proposed (e.g. [3, 7, 19, 29]), together to a parametrization of the rotation group based on the exponential map and the rotation vector; these procedures aimed to study the rotational motion of a rigid body, and to evaluate the dynamic response of 3D beam elements. The main difficulty consists in the fact that standard time-stepping procedure such as the Newmark scheme, are based on a linear interpolation; this operation is well defined only if the interpolated quantities belong to the same linear space.

By the procedure previously introduced, all the variables adopted at the structural level (namely the pseudo vector of rotation, its additive variation and its derivatives with respect to time) lie in the same tangent space $T_I SO(3)$, because all the transformations allowing for a spatial representation of the rotational motion of the section are accomplished at the element level. As a consequence, the proposed procedure allows for adopting a standard Newmark time stepping scheme for the integration of the equation of motion, both for the rotational as for the translational global nodal parameters.

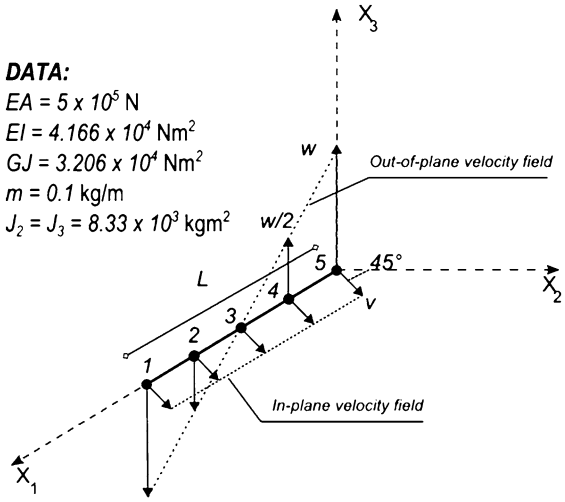

Fig. 4 Free beam. Finite element mesh and initial velocity field

5 Numerical application

5.1 Free beam in helicoidal motion

As a first example, we study the free motion of the beam represented in Fig. 4. The initial velocity field generates a nearly rigid helicoidal motion, about a revolution axis passing through the midpoint of the beam and parallel to the bisection axis of the plane (X_1, X_2). Under the rigid body motion assumption, the constant translational velocity is equal to the initial in-plane velocity v, while the angular velocity of the beam, ω, can easily be related to the initial out of plane velocity of the beam end points, w. This is a significant test that stresses both the kinematic description and the

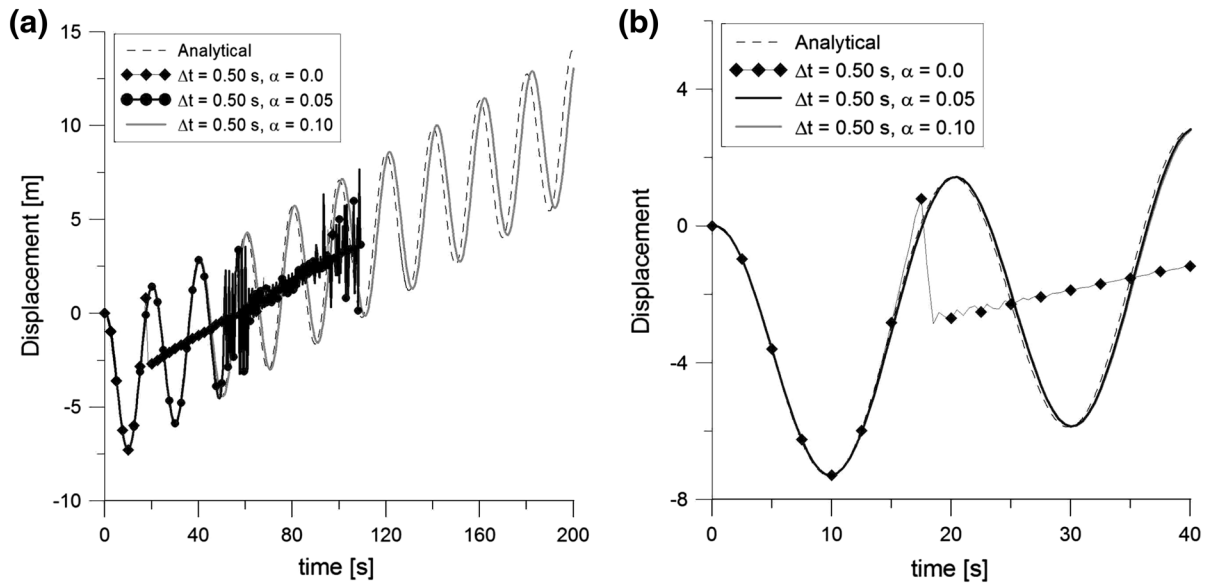

Fig. 5 Node 5. $\Delta t = 0.50$ s. **a** Displacements in direction X_1. **b** Enlargement of figure (**a**)

numerical integration scheme. In fact, to correctly predict the response of the structure, they have to be able to follow the path of material points through a large number of revolutions.

Numerical results are here compared to the analytical solution, showing the ability of the proposed finite element formulation in describing a large three-dimensional motion.

To this aim, we considered a beam with length $L = 8$ m. The material is linearly elastic. Stiffness and mass parameters are listed in Fig. 4. The initial velocity field is characterized by the values: $v = 0.1\text{m/s}$ and $w = 0.4 \times \pi\text{m/s}$. The rigid body angular velocity, ω, and the initial kinetic energy, T_0, corresponding to these assumptions are equal to: $\omega = 0.1 \times \pi\text{rad/s}$ and $T_0 = 0.21\text{J}$.

Computations have been performed by adopting a mesh of four equally spaced elements (see Fig. 4), and the rotation update procedure based on the complete trigonometric expression of the incremental rotation tensors (CFUL rotation update procedure). The performances of the standard trapezoidal Newmark algorithm ($\beta = 0.25$, $\gamma = 0.50$) have been compared to those of the well known HHT scheme [16] for different values of the numerical dissipation parameter α and of the time step, Δt.

The displacement time histories in direction X_1 of the end node 5, evaluated with time step $\Delta t = 0.5$ s and $\Delta t = 0.25$ s are shown, respectively, in Figs. 5 and 6.

In both cases the standard Newmark integration scheme ($\alpha = 0$) leads to numerical instability, which is related, as can be inferred from Fig. 7, to an unbounded growth of the kinetic energy of the system. This phenomenon is related to the numerical integration of the rotational component of the motion. Indeed, the translational component of the motion is well captured also after the onset of the instability, as can be noticed from Figs. 6 and 7.

As shown in Figs. 5 and 6 the numerical instability can be avoided introducing a suitable amount of numerical dissipation by adjusting the parameter α of the HHT integration scheme. As a final note, analysis of the results shows that kinetic energy is very well conserved by the proposed formulation (see Fig. 7) over very long simulation periods, beside the very small dissipation due to adoption of the HHT method. At the end of the simulation for $\Delta t = 0.25$ s, relative energy loss was of the order of 1.4×10^{-3} for $\alpha = 0.05$ and 4.7×10^{-4} for $\alpha = 0.10$.

5.2 Large 3D oscillation of a right angle cantilever

In this section we consider a well known benchmark case, a rightangle cantilever (Fig. 8) subjected to an out-of-plane load applied at the elbow (point B),

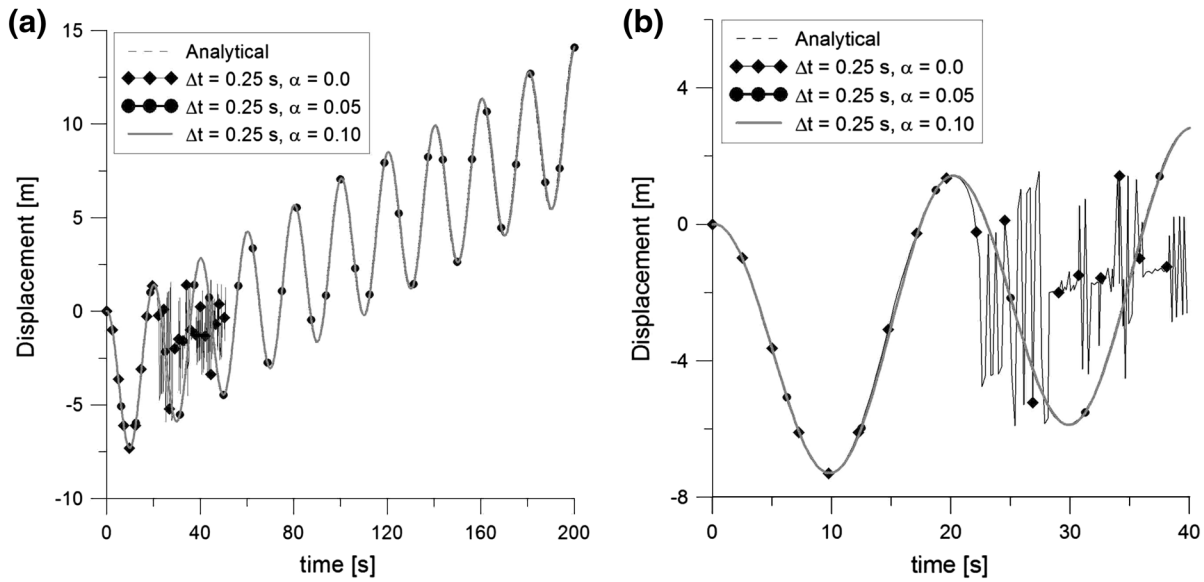

Fig. 6 Node 5. $\Delta t = 0.25$ s. **a** Displacements in direction X_1. **b** Enlargement of figure (**a**)

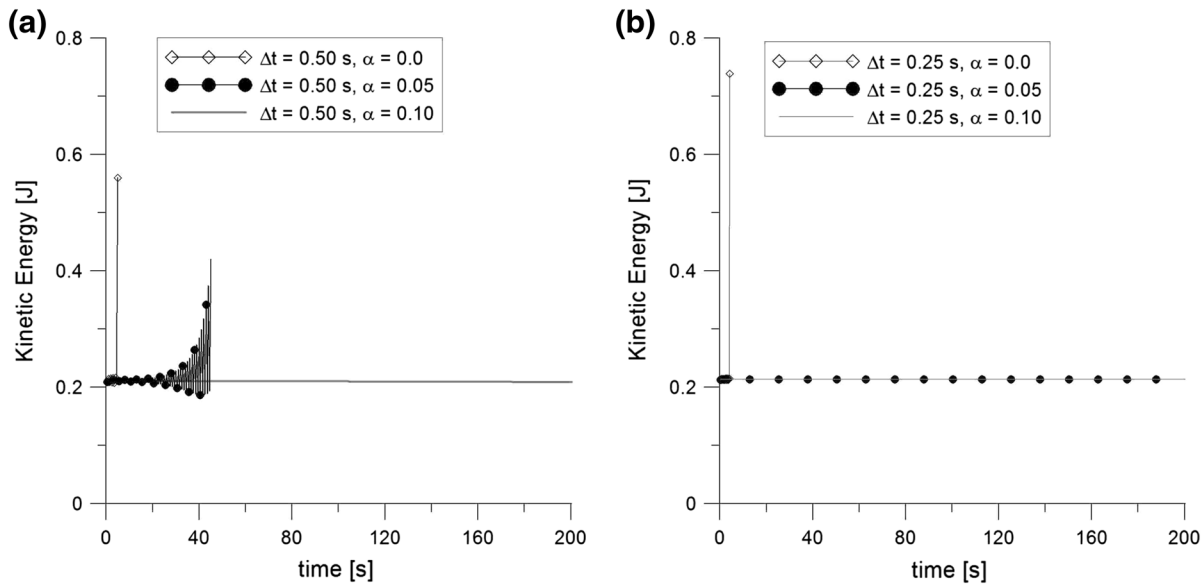

Fig. 7 Kinetic energy of the finite element model. **a** $\Delta t = 0.50$ s. **b** $\Delta t = 0.25$ s

already studied by Mata et al. in [22] and also in [12], to which we apply the computational procedure of the inertia forces previously described. After the application of the load, the structure undergoes free vibrations with coupled contributions from large bending and twisting displacements, that are all of the order of magnitude of the frame size. The example is of interest, being a dynamic case involving a highly spatial motion and large rotations for the frame members. The geometrical non linearities imply that the response is controlled by the coupling among all the "elementary" structural behaviors of the frame members. The material is assumed linearly elastic. Stiffness and mass parameters are listed in Fig. 8.

First of all, we show a comparison among the results obtained with three different discretizations of

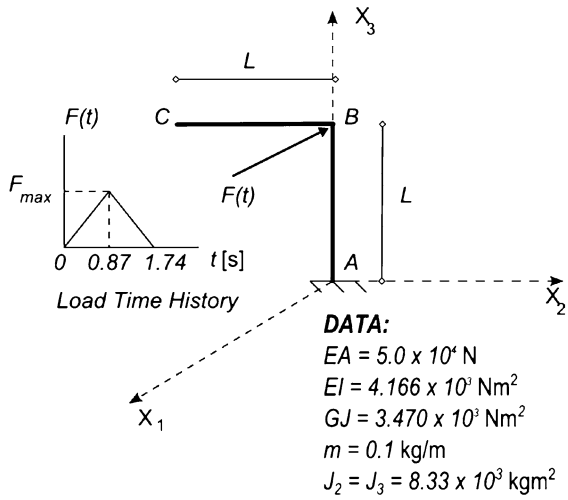

Fig. 8 Right angle cantilever and load time history

the structure, namely: 10, 20 and 100 equally spaced elements.

In all cases, five Gauss-Lobatto sections are adopted to evaluate the restoring forces and the tangent (static) stiffness matrix of the elements, as well as the rotational contribution to the element inertia forces and tangent mass matrix. Large nodal rotations are accounted for by exploiting the updated lagrangian procedure based on the evaluation of the incremental rotation matrix performed by means of the complete trigonometric expression (CFUL update procedure).

The equations of motion have been integrated by adopting a standard implicit Newmark algorithm with time step $\Delta t = 0.03$ s and time-stepping parameters $\beta = 0.25$ and $\gamma = 0.50$; a full Newton–Raphson has been employed to solve the non-linear problem at each step of the dynamic analysis.

Results are shown in Fig. 9 in terms of the out of plane displacement time-histories of the elbow and of the tip. The results presented in [22] are also shown for comparison. Refining the mesh, the results obtained for different discretizations, which are partially shown in Fig. 9, tend to converge to the curve shown for 100 elements. By furtherly doubling the number of elements practically no differences are detected. Some differences can still be detected with the curves by [22]. In this respect, it can be noticed that during the first part of the response, in which the load is acting and the response of the structure is governed by the bending of the column, all the models deliver practically the same results. This holds true irrespectively of the adopted discretization, which has probably a significant effect in the second part of the response, where free vibration occurs. In this respect, the behaviour of the model in [22], which is implemented with a coarse mesh (6 elements) in the computation shown in [22], cannot be inferred here. In addition, some tests performed show that the free

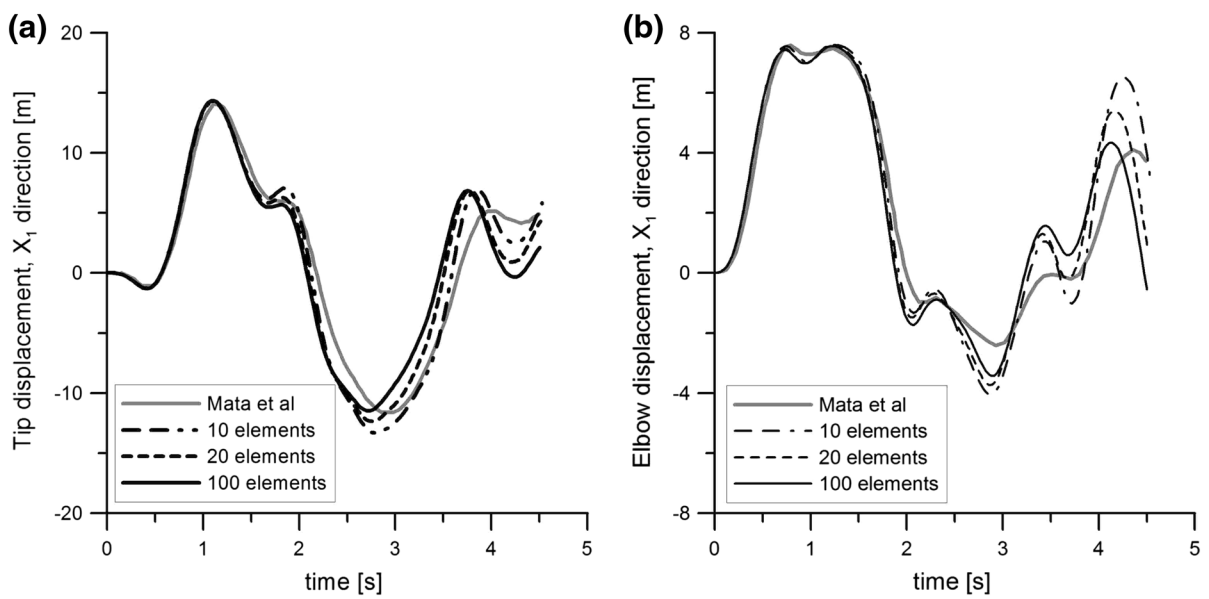

Fig. 9 CFUL with different discretizations. **a** Tip, **b** elbow displacement

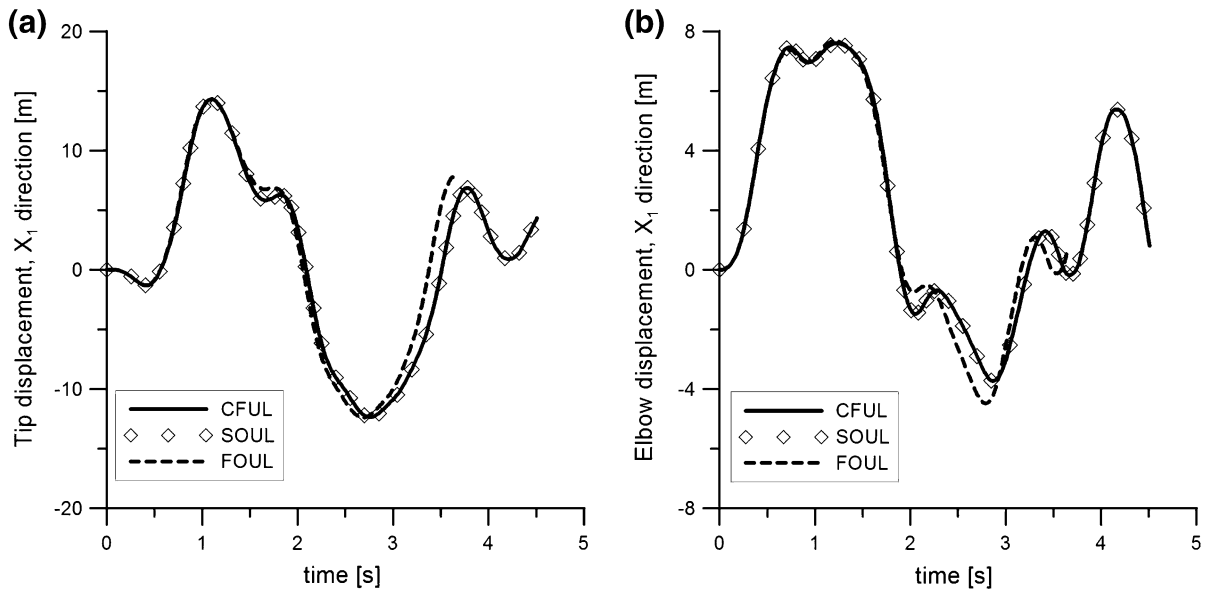

Fig. 10 20-elements mesh with different rotation update strategies. **a** Tip, **b** elbow

vibration response ($t > 1.8$ s) is very sensitive to the modelling of the torsional stiffness of the members, which do not affect significantly the loading phase.

In the following a comparison is also given among results obtained with different update strategies of rotations, namely the CFUL update procedure and the first order and second order approximate procedures FOUL and SOUL described in Sect. 2; to this aim in Fig. 10 we show the out of plane displacement time-histories of the elbow and of the tip obtained for the different rotation update strategies obtained with the 20-elements mesh. CFUL and SOUL give practically the same results, while the FOUL procedure, as expected, delivers a less accurate response. In fact, truncating the exponential map of the incremental rotation tensor to the first order implies enforcing the hypothesis of small incremental nodal rotations. This leads to numerical errors which accumulate from step to step, and finally significantly affect the results. Moreover, the accumulation of errors leads to the failure of the analysis after about 3.5 seconds.

Numerical simulation have been also performed on a time interval of 200 s, by considering the CFUL update procedure, and an HHT integration scheme, with a numerical dissipation parameter $\alpha = 0.10$. The proposed approach allows to capture the periodic steady state vibrations of the structure, avoiding both the numerical problem related to an approximate description of

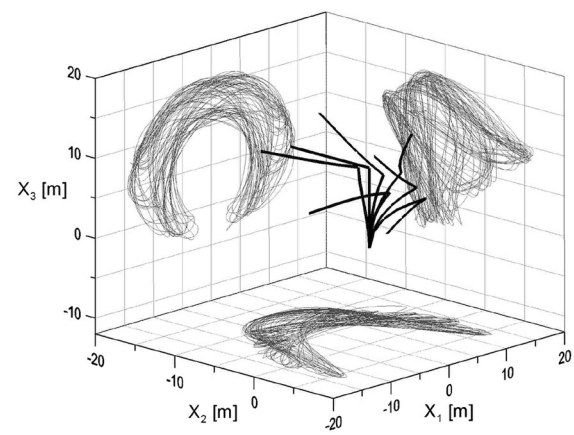

Fig. 11 10 element-mesh: CFUL with $\alpha = 0.10$. Projections of the tip displacements and some representative *deformed shapes* of the frame

nodal rotations as well as the numerical instabilities related to the standard Newmark scheme. As an example, the projections of the tip displacement evaluated with the 10-elements are shown in Fig. 11 together to some representative deformed shapes of the structure.

6 Conclusions

In this paper geometrically exact and corotational approaches are combined in the formulation of a 3D

beam element to study the dynamic response in large displacements and rotations, aiming at exploiting the advantages of both formulations while, at the same time, eliminating some of their drawbacks.

In this context, a corotational beam finite element , previously developed within the authors research group for the study of the structural response of flexible structures, is adopted as the base of the proposed formulation to compute the nodal restoring forces.

The inertia forces are computed adopting a newly proposed procedure . The evaluation of the beam inertia forces is based on the exact description of the element cross sections kinematics, so to avoid the approximations related to classic corotational formulations.

The subject of integration of equations of motion has been addressed taking into account the non-linear character of the element configuration space, which is due to the presence of large rotations. Within this context, the proposed procedure has been shown able to correctly operate with standard time stepping schemes, with practical advantages on the reuse of well established numerical algorithms.

The proposed procedure has been compared with good results to some significant cases which imply both large rigid body motions and a complex deformed state involving displacements due to bending and torsion of the order of magnitude of the dimension of the structure. The results highlight the soundness of the proposed formulation based on splitting the description of the static and inertia forces of the element.

Appendix: evalution of the corotational transformation matrix

In order to evaluate the corotational transformation matrix, $\boldsymbol{T}$, let us introduce first some preliminary results. Consider first the variation of the unit chord vector of the beam element, $\boldsymbol{e}_1$, whose definition is given in Eq. (21). Denoting as $\delta\boldsymbol{d}_1$ and $\delta\boldsymbol{d}_2$ the variations of the nodal translation vectors, the following holds:

$$\delta\boldsymbol{e}_1 = \boldsymbol{C}_{e1}\delta\boldsymbol{d}_2 - \boldsymbol{C}_{e1}\delta\boldsymbol{d}_1 \tag{46}$$

where, adopting the symbol $\boldsymbol{I}$ for the identity (3×3) matrix, and $\otimes$ to denote the dyadic product:

$$\boldsymbol{C}_{e1} = \frac{\boldsymbol{I} - \boldsymbol{e}_1 \otimes \boldsymbol{e}_1}{\|\boldsymbol{x}_2 - \boldsymbol{x}_1\|} = \frac{\boldsymbol{I} - \boldsymbol{e}_1 \otimes \boldsymbol{e}_1}{L} \tag{47}$$

Equation (46) can be rewritten concisely as:

$$\delta\boldsymbol{e}_1 = \boldsymbol{A}_1\delta\boldsymbol{q} \tag{48}$$

where, denoting as $\boldsymbol{0}$ the (3×12) zero matrix, we have introduced $\boldsymbol{A}_1$ as:

$$\boldsymbol{A}_1 = (-\boldsymbol{C}_{e1}, \boldsymbol{C}_{e1}, \boldsymbol{0}, \boldsymbol{0}) \tag{49}$$

Now we consider the variation of the vectors of the Cartesian bases: $\left\{\boldsymbol{b}_i^{(j)}\right\}$, $j = 1, 2$. Denoting as $\delta\boldsymbol{\Lambda}^{(j)}$ the virtual variations of the j-th nodal rotation tensor, the following expression can be introduced:

$$\delta\boldsymbol{b}_i^{(j)} = \delta\boldsymbol{\Lambda}^{(j)}\,\boldsymbol{b}_i^{(j)}, i = 1, 2, 3,\ j = 2, 3 \tag{50}$$

which, exploiting the properties of the skew-symmetric operator $\boldsymbol{S}()$, can be also be rewritten (see [13] for further details) as:

$$\delta\boldsymbol{b}_i^{(j)} = \boldsymbol{B}_i^{(j)}\,\delta\boldsymbol{q}, i = 1, 2, 3,\ j = 2, 3 \tag{51}$$

with the definitions:

$$\boldsymbol{B}_i^{(1)} = \left(\boldsymbol{0}, \boldsymbol{0}, -\boldsymbol{S}\left(\boldsymbol{b}_i^{(1)}\right)\boldsymbol{H}(\boldsymbol{\phi}_1), \boldsymbol{0}\right), i = 1, 2, 3 \tag{52}$$

and:

$$\boldsymbol{B}_i^{(2)} = \left(\boldsymbol{0}, \boldsymbol{0}, \boldsymbol{0}, -\boldsymbol{S}\left(\boldsymbol{b}_i^{(2)}\right)\boldsymbol{H}(\boldsymbol{\phi}_2)\right), i = 1, 2, 3 \tag{53}$$

By exploiting the definitions of matrices $\boldsymbol{A}_1$ and $\boldsymbol{B}_i^{(j)}$, the virtual variations of the local displacements can be expressed in closed form as follows (see [13] for further details):

$$\delta e = -\boldsymbol{e}_1{}^T\delta\boldsymbol{d}_1 + \boldsymbol{e}_1{}^T\delta\boldsymbol{d}_2 = \left(-\boldsymbol{e}_1{}^T, \boldsymbol{e}_1{}^T, \boldsymbol{0}, \boldsymbol{0}\right)\delta\boldsymbol{q} \tag{54}$$

$$\delta\theta_t = \delta\boldsymbol{b}_3^{(1)T}\boldsymbol{b}_2^{(2)} + \boldsymbol{b}_3^{(1)T}\delta\boldsymbol{b}_2^{(2)} = \left(\boldsymbol{b}_2^{(2)T}\boldsymbol{B}_3^{(1)} + \boldsymbol{b}_3^{(1)T}\boldsymbol{B}_2^{(2)}\right)\delta\boldsymbol{q} \tag{55}$$

$$\delta\theta_i^{(j)} = k\,\delta\boldsymbol{b}_{i+k}^{(j)T}\,\boldsymbol{e}_1 + k\,\boldsymbol{b}_{i+k}^{(j)T}\,\delta\boldsymbol{e}_1 = k\left(\boldsymbol{e}_1^T\boldsymbol{B}_{i+k}^{(j)} + \boldsymbol{b}_{i+k}^{(j)T}\boldsymbol{A}_1\right)\delta\boldsymbol{q} \tag{56}$$

with: $k = (-1)^i j = 1, 2,\ i = 2, 3$. From above, the six columns of the corotational transformation matrix, $\boldsymbol{T}$, from $\delta\boldsymbol{q}$ to the virtual variations of local displacements, $\delta\boldsymbol{p}$, can be defined as:

$$\boldsymbol{t}_1 = \left(-\boldsymbol{e}_1{}^T, \boldsymbol{e}_1{}^T, \boldsymbol{0}, \boldsymbol{0}\right)^T \tag{57}$$

$$\boldsymbol{t}_2 = \left(\boldsymbol{b}_2^{(2)\,T}\boldsymbol{B}_3^{(1)} + \boldsymbol{b}_3^{(1)\,T}\boldsymbol{B}_2^{(2)}\right)^T \tag{58}$$

$$\boldsymbol{t}_{j+i} = k\left(\boldsymbol{e}_1^T\boldsymbol{B}_{i+k}^{(j)} + \boldsymbol{b}_{i+k}^{(j)T}\boldsymbol{A}_1\right)^T \tag{59}$$

With: $k = (-1)^i, j = 1,\ i = 2, 3$.

$$\boldsymbol{t}_{j+i+1} = k\left(\boldsymbol{e}_1^T\boldsymbol{B}_{i+k}^{(j)} + \boldsymbol{b}_{i+k}^{(j)T}\boldsymbol{A}_1\right)^T \tag{60}$$

With: $k = (-1)^i, j = 2,\ i = 2, 3$.

References

1. Argyris J (2002) An excursion into large finite rotations. Comput Methods Appl Mech Eng 32:85–155
2. Battini JM, Pacoste C (2002) Co-rotational beam elements with warping effects in instability problems. Comput Methods Appl Mech Eng 191:1755–1789
3. Cardona A, Geradin M (1989) Time integration if the equations of motion in mechanism analysis. Comput Struct 33:801–820
4. Cardona A, Geradin M (1988) A beam finite element non linear theory with finite rotations. Int J Numer Methods Eng 26:2403–2438
5. Choquet-Bruhat Y, Dewitte-Morette C, Dillard-Bleick M (1997) Analysis manifolds and physics. North Holland, Amsterdam
6. Crisfield MA (1997) Non linear finite element analysis of solids and structures. Advanced topics. Wiley, New York
7. Crisfield MA, Galvanetto U, Jelenic G (1997) Dynamics of 3-D co-rotational beams. Comput Mech 20:507–519
8. Crisfield MA, Jelenic G (1999) Geometrically exact 3D beam theory: implementation of a strain-invariant finite element for statics and dynamics. Comput Methods Appl Mech Eng 171:141–171
9. Di Pilato M, Martelli F, Martinelli L (2007) Corotational cable elements for the study of fluid-structure interaction. In: Proceedings of the 7th International Symposium on Cable Dynamics, Vienna, December 10–13
10. Di Pilato M, Martelli F, Martinelli L (2009) Corotational cable elements to model suspended cables under wind loading. In: Proceedings of the 5th EACWE—European and African conference on wind engineering, Florence, July 10–23
11. Foti F, Martinelli L (2013) A corotational beam element to model the hysteretic bending behavior of metallic wire ropes. In: Proceedings of The 4th Canadian conference on nonlinear solid mechanics (CanCNSM 2013), Montreal, July 23–26
12. Foti F, Martinelli L (2012) Dynamics of corotational beam elements in large displacements and rotations—some aspects on the kinetic energy and the integration of the equations of motions. In: Proceedings of the 6th European congress on computational methods in applied sciences and engineering (ECCOMAS 2012), Vienna, September 10–14
13. Foti F (2013) A corotational beam element and a refined mechanical model for the nonlinear dynamic analysis of cables. Doctoral Dissertation, Politecnico di Milano, Milano
14. Felippa CA, Haugen B (2005) A unified formulation of small-strain corotational finite elements: I. theory. Comput Methods Appl Mech Eng 194:2285–2335
15. Geradin M, Rixen D (1995) Parametrization of finite rotations in computational dynamics: a review. Rev Eur Ele Fin 4:497–553
16. Hilber HM, Hughes TJR, Taylor RL (1977) Improved numerical dissipation for time integration algorithms in structural dyanmics. Earthq Eng Struct Dyn 5:283–292
17. Hsiao KM, Lin JY, Lin WY (1999) A consistent co-rotational finite element formulation for geometrically nonlinear dynamic analysis of 3-D beams. Comput Methods Appl Mech Eng 169:1–18
18. Le TN, Battini JM, Hjiaj M (2014) A consistent 3D corotational beam element for nonlinear dynamic analysis of flexible structures. Comput Methods Appl Mech Eng 269:538–565
19. Makinen J (2001) Critical study of Newmark-scheme on manifold of finite rotations. Comput Methods Appl Mech Eng 191:818–828
20. Makinen J (2008) Rotation manifold SO(3) and its tangential vectors. Comput Mech 42:907–919
21. Mata P, Oller S, Barbat AH (2007) Static analysis of beam structures under nonlinear geometric and costitutive behavior. Comput Methods Appl Mech Eng 196:4458–4478
22. Mata P, Oller S, Barbat AH (2008) Dynamic analysis of beam structures considering geometric and constitutive nonlinearity. Comput Methods Appl Mech Eng 197:857–878
23. Meek JL, Tan HS (1984) Geometrically nonlinear analysis of space frames by an incremental iterative technique. Comput Methods Appl Mech Eng 47:261–282
24. Oran C (1973) Tangent stiffness in space frames. ASCE J Struct Div 99:987–1001
25. Pacoste C, Eriksson A (1997) Beam elements in instability problems. Comput Methods Appl Mech Eng 144:163–197
26. Rankin CC, Brogan FA (1986) An element-independent corotational procedure for the treatment of large rotations. ASME J Press Vessel Technol 108:165–174
27. Simo JC (1985) A finite strain beam formulation. The three-dimensional dynamic problem. Part I. Comput Methods Appl Mech Eng 49:55–77
28. Simo JC, Vu-Quoc L (1986) A three-dimensional finite-strain rod model. Part II: computational aspects. Comput Methods Appl Mech Eng 58:79–116
29. Simo JC, Wong K (1991) Unconditionally stable algorithms for rigid body dynamics that exactly preserve energy and momentum. Int J Numer Methods Eng 31:19–52
30. Spurrier RA (1978) Comment on singularity-free extraction of a quaternion from a direction cosine matrix. J Spacecr Rockets 15:255
31. Wasfy TM, Noor AK (2003) Computational strategies for flexible multibody systems. Appl Mech Rev 56:553–613